ac-driven annular Josephson junctions: The missing Shapiro steps

I. R. Rahmonov,[1,2] J. Tekić,[3] P. Mali,[4] A. Irie,[5] and Yu. M. Shukrinov[1,6]
[1]BLTP, JINR, Dubna, Moscow Region 141980, Russia
[2]Umarov Physical Technical Institute, TAS, Dushanbe 734063, Tajikistan
[3]"Vinča" Institute of Nuclear Sciences, Laboratory for Theoretical and Condensed Matter Physics - 020, University of Belgrade, PO Box 522, 11001 Belgrade, Serbia
[4]Department of Physics, Faculty of Science, University of Novi Sad, Trg Dositeja Obradovića 4, 21000 Novi Sad, Serbia
[5]Department of Electrical and Electronic Systems Engineering, Utsunomiya University, 7-1-2 Yoto, Utsunomiya 321-8585, Japan
[6]Dubna State University, Dubna 141980, Russia

(Received 10 October 2019; published 21 January 2020)

Examination of an annular system of underdamped Josephson junctions in the presence of external radiation showed that the ability of the system to lock with some external radiation was determined not only by the number but also by the type of rotating excitations (fluxons or antifluxons). Shapiro steps can be observed in the current-voltage characteristic only in the system with trapped fluxons or in the system with fluxon-antifluxon pairs. If the trapped fluxons circulate simultaneously with fluxon-antifluxon pairs, there are no Shapiro steps regardless of the amplitude or frequency of the applied external radiation.

DOI: 10.1103/PhysRevB.101.024512

I. INTRODUCTION

The idea that a fluxon behaves as a particlelike solitary wave, which can be manipulated and controlled, motivated creation of a logic circuit by using Josephson fluxon as elementary bits of information [1–7]. In the creation of new logic elements, particularly important are the long Josephson junctions [8] described by a continuous sine-Gordon (SG) equation, and the Josephson junctions parallel array by its discreet counterpart, i.e., the Frenkel-Kontorova model [8–12]. However, in long Josephson junctions (JJs), the motion of fluxon strongly depends on the geometry and boundaries of the junctions, which makes studies of fluxon dynamics very challenging. These problems led to the creation of annular Josephson junctions [13] as ideal systems for the studies of fluxon dynamics, which provide an undisturbed and tunable fluxon motion [14–21].

One of the most interesting properties of Josephson junction systems is their ability to exhibit various resonance phenomena. In the absence of any external radiation, the so-called *zero-field steps* (ZFSs) [11,22,23] appear in the current-voltage (I-V) characteristic due to resonant motion of fluxons and antifluxons inside the system. If, on the other hand, some external radiation is applied, the I-V characteristic exhibits the well-known *Shapiro steps* [24] as a result of the locking with the external frequency. When the locking appears at the integer values of external frequency, the steps are called harmonics, while the locking at rational noninteger values leads to subharmonics (for the locking at the half-integer values of external frequency, the steps are called half-integer steps) [10]. Though the Shapiro steps are today one of the most recognized frequency locking phenomena associated with a wide variety of physical systems [10], the majority of the works [14–21] on annular Josephson junctions have been focused on the resonance phenomena in the absence of external radiation.

In this study, we will examine the underdamped dynamics of an annular array of Josephson junctions (AAJJs) under the external radiation. In contrast to previous studies of annular Josephson junctions, which were mainly focused on the case of one trapped fluxon in a small range of currents and voltages [14,15], here we will examine the Shapiro steps in various cases of circulating excitations (fluxons and antifluxons), in a wide range of currents and voltages in order to get the full picture of dynamical behavior. Surprisingly, our results show that ability of the system to lock with some external radiation depends not only on the number but also on the type of excitations, i.e., whether there are only trapped fluxons or the fluxon-antifluxon pairs in the system, or the trapped fluxons circulate simultaneously with fluxon-antifluxon pairs.

II. MODEL

We consider an annular parallel array of N Josephson junctions in the underdamped regime presented in Fig. 1. The total length of a chain is $L = Na$, where a is a distance between the neighboring junctions. The annular system that we are considering here can be described by the discrete version of perturbed sine-Gordon equation, which is well known as the dissipative Frenkel-Kontorova model [9]:

$$\frac{d^2\varphi_i}{dt^2} - \frac{\varphi_{i+1} + 2\varphi_i + \varphi_{i-1}}{a^2} + \sin\varphi_i + \alpha\frac{d\varphi_i}{dt} = I + A\sin(\omega t), \tag{1}$$

where φ_i is the phase difference across the ith junction, α is the dissipation parameter, I is the total or biased current through the junction, and A and ω are the amplitude and frequency of external radiation, respectively. The coupling between the neighboring junctions is described by the constant $\frac{1}{a^2}$, where $a = \sqrt{2\pi L_0 I_c/\Phi_0}$ is the discreteness parameter, i.e., the distance between two junctions normalized to the Josephson

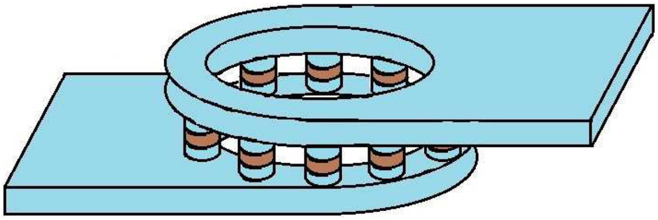

FIG. 1. Schematic view of an annular array of Josephson junctions. The junctions are colored in dark red.

penetration depth. The time is normalized with respect to the inverse plasma frequency ω_p^{-1}, where $\omega_p = \sqrt{2\pi I_c/(\Phi_0 C)}$, I_c is the critical current, L_0 and C are the inductance and capacitance of single cell, respectively, and $\Phi_0 = \frac{h}{2e}$ is the flux quantum [25].

The Frenkel-Kontorova model or the discrete SG model takes into consideration only inductive interaction between the neighboring junctions. Capacitive interaction, on the other hand, was taken into account in the FCU (Fistul, Caputo, and Ustinov) model in Ref. [26]. Later, a comparative analysis between the two models (the discrete SG model and the FCU model) and the experimental results was performed in an annular system of Josephson junctions in Ref. [14]. The authors showed that both the discrete SG model and the FCU model agreed very well with experiments. The influence of capacitive interaction was negligible, which led to the conclusion that the conventional discrete SG model was good enough to describe the experiments.

In order to calculate the *I-V* characteristic of the AAJJs we have used Eq. (1) and the Josephson relation:

$$V_i = \frac{d\varphi_i}{dt} = \omega_J, \tag{2}$$

where V_i is the voltage of the ith junction normalized to $V_0 = \hbar\omega_p/2e$, and ω_J is the Josephson frequency normalized to ω_p.

Our numerical simulations were performed for the periodic boundary conditions, which in discrete case have the form

$$\varphi_{N+1} = \varphi_1 + 2\pi M, \quad \varphi_0 = \varphi_N - 2\pi M, \tag{3}$$

where M is the number of trapped fluxons inside the system. The spatial points $i = 0$ and $i = N + 1$ were assumed to be equivalent to $i = N$ and $i = 1$, respectively. We have applied the well-known procedure used in Refs. [27,28]. The current was changed by step ΔI and for every value of I the corresponding voltage V was calculated; in that way, the *I-V* characteristic was produced. We note that the solution at a certain value of I was used as the initial condition for the calculation of the next point at the value of bias current $I + \Delta I$.

III. RESULTS

If no trapped fluxons are present in the system ($M = 0$), one or more fluxon-antifluxon pairs, which appear as a soliton solution of a dynamical equation, are circulating along the system. Due to the presence of external radiation, in addition to zero-field steps, the system will also exhibit Shapiro steps. In Fig. 2 the *I-V* characteristic of the AAJJs in the presence

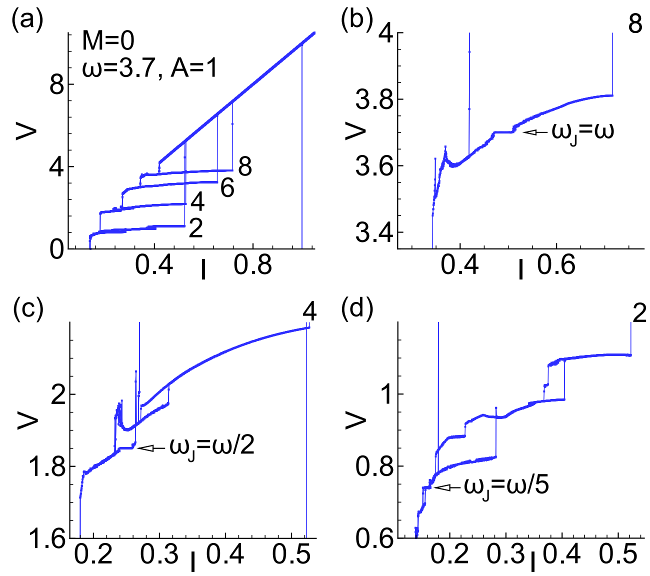

FIG. 2. (a) The current-voltage characteristic of the annular array of Josephson junctions for $N = 10$, $a = 1$, $\alpha = 0.1$, and $M = 0$. The amplitude and frequency of external radiation are $A = 1$ and $\omega = 3.7$, respectively. The units for I, V and ω are normalized to $I_c = 50\,\mu$A, $V_0 = 0.61$ mV and $\omega_p = 1.857$ THz, respectively. The numbers 2, 4, 6, and 8 mark the total number of fluxons and antifluxons n. The zoomed parts of I-V characteristic correspond to: (b) the harmonic step on the ZFS $n = 8$; (c) the halfinteger step on the ZFS $n = 4$; and (d) the subharmonic step $\frac{1}{5}$ on the ZFS $n = 2$.

of external radiation for $M = 0$ is presented. The units for I, V, and ω are dimensionless and normalized to $I_c = 50\ \mu$A, $V_0 = 0.61$ mV, and $\omega_p = 1.857$ THz, respectively, so that our analyses have been performed in the experimentally relevant regions of currents and voltages [14]. At first, it might appear in Fig. 2(a) that the *I-V* characteristic exhibits only four ZFSs, which appear when V, i.e., the Josephson frequency, satisfies the resonant condition $V = \omega_J = \frac{2\pi n u}{L}$, where u is a speed of moving fluxon (antifluxon). Considering that $V \sim n$, the *I-V* characteristic clearly shows that these steps correspond to $n = 2,\ 4,\ 6,$ and 8. Here, $n = n_f + n_{af} = 2n_p + M$ is the total number of excitations, i.e., fluxons and antifluxons in the system, where n_f, n_{af}, and n_p are the number of fluxons, antifluxons, and fluxon-antifluxon pairs, respectively. Since our system is topologically closed M must be conserved, and consequently for $M = 0$ the excitations appear only in the form of fluxon-antifluxon pairs. However, the high-resolution analysis reveals also the Shapiro steps that come from the locking of Josephson frequency and the frequency of external radiation. For a given external frequency $\omega = 3.7$, the first harmonic step appears on the $n = 8$ ZFS as can be seen in Fig. 2(b), while Figs. 2(c) and 2(d) show the half integer $\frac{1}{2}\omega$ and the subharmonic step $\frac{1}{5}\omega$, which appear on the $n = 4$ and $n = 2$ ZFS, respectively. We have examined the AAJJs for a wide range of applied frequencies ω, and we were able to obtain Shapiro steps in the whole area of the *I-V* characteristic in Fig. 2.

If there are fluxons trapped in the system, the ability of the system to exhibit Shapiro steps will completely change.

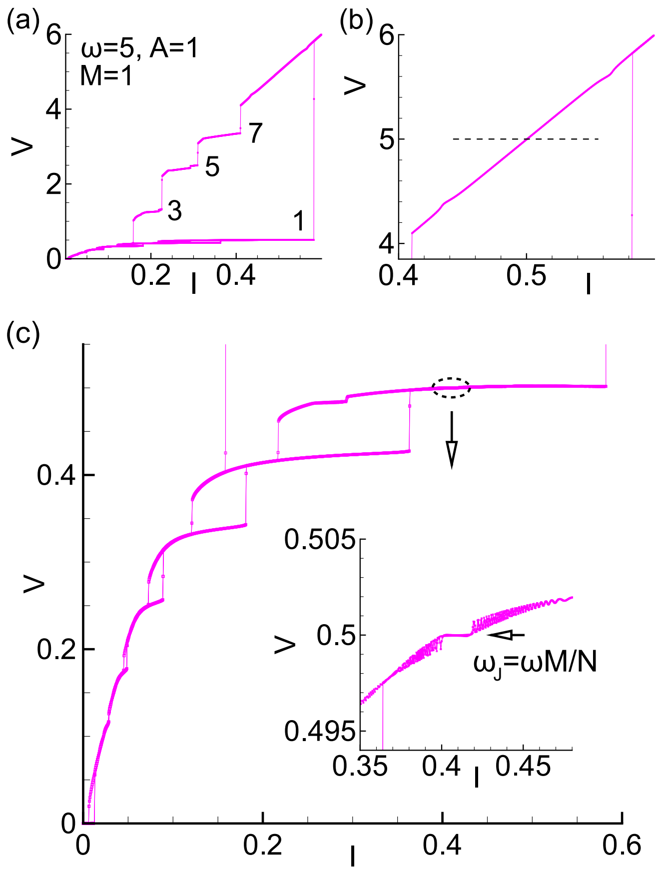

FIG. 3. (a) The current-voltage characteristic of the annular array of Josephson junctions for $M = 1$, with the amplitude and frequency of external radiation $A = 1$ and $\omega = 5$, respectively. The rest of the parameters are the same as in Fig. 2. The numbers 1, 3, 5, and 7 mark the total number of fluxons and antifluxons n. (b) The absence of the Shapiro step in the I-V curve. Dashed line marks where the step should be. (c) High-resolution plot of the step $n = 1$, which exhibits Shapiro step shown in the inset.

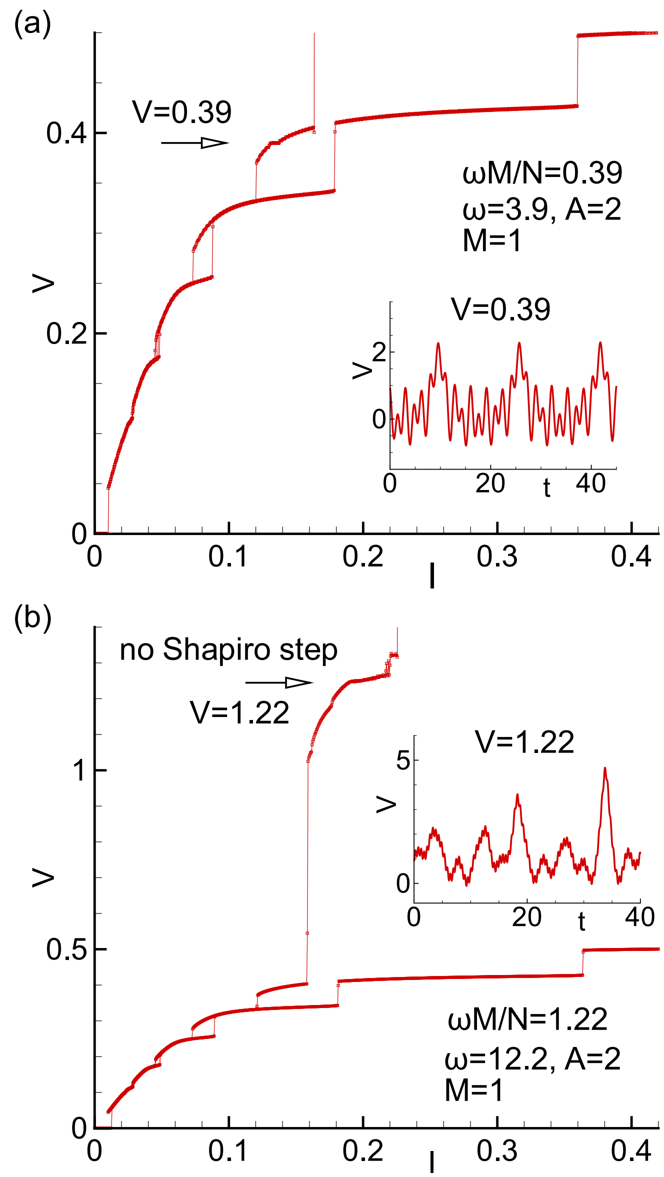

FIG. 4. (a) The part of the I-V characteristic corresponding to the step $n = 1$ for $M = 1$, $\omega = 3.9$, $A = 2$. The rest of the parameters are the same as in Fig. 2. (b) The part of the I-V characteristic corresponding to the $n = 3$ ZFS for $M = 1$, $\omega = 12.2$, $A = 2$. Insets show the voltage-time dependence at the values of I marked by arrows at which Shapiro steps should appear.

In Fig. 3 the I-V characteristic of the AAJJ with one trapped fluxon ($M = 1$) is presented. Since in addition to the one trapped fluxon, which is introduced through the boundary condition in Eq. (3), the additional excitations appear only in the form of fluxon-antifluxon pairs the system exhibits ZFSs for $n = 1,\ 3,\ 5$, and 7. In this case, for the applied frequency of the external radiation $\omega = 5$, in Fig. 3(a) we would expect to see the Shapiro step at $V = 5$ as well as other subharmonic steps in the I-V characteristic. However, as we can see in Fig. 3(b) there is no Shapiro step, and the only Shapiro step we could detect was the step $\frac{1}{10}\omega$, which appears for $n = 1$ in Fig. 3(c). We have to point out that while for the case $M = 0$ in Fig. 2 Shapiro steps appear due to locking between the Josephson frequency and the frequency of external radiation, i.e., always when ω_J is equal to some rational (integer or non-integer) number of ω, in the case of trapped fluxons (see, e.g., $M = 1$ in Fig. 3), the trapped fluxons introduce an additional time scale, and Shapiro steps come due to locking between the frequency of circulating fluxons and the frequency of external radiation, in which case the condition for their appearance, $\omega_J = \frac{M\omega}{N}$, is also determined by the number of trapped fluxons M and the number of junctions N.

In Fig. 4 two I-V characteristics at two different values of applied frequencies are presented. As in the previous case, the Shapiro step appears in Fig. 4(a) at $V = 0.39$, when the applied frequency is in the region of the step $n = 1$, i.e., in the region where only one trapped fluxon rotates through the system. On the other hand, if we increase the frequency to the value, which corresponds to the higher steps ($n > 1$) in I-V characteristic, no Shapiro steps appear as can be seen for $V = 1.22$ at the $n = 3$ step in Fig. 4(b). The voltage-time dependence given in the insets clearly shows the periodic

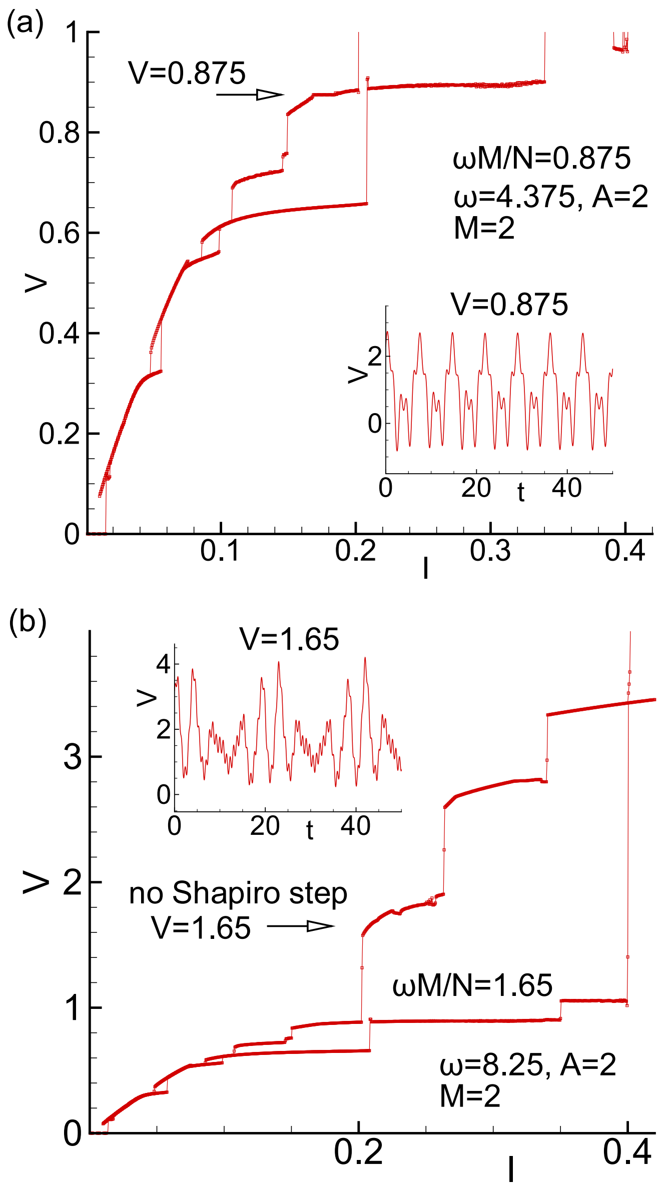

FIG. 5. (a) The part of the I-V characteristic corresponding to the step $n = 2$ for $M = 2$, $\omega = 4.375$, $A = 2$. The rest of the parameters are the same as in Fig. 2. (b) The part of the I-V characteristic corresponding to the step $n = 4$ for $M = 2$, $\omega = 8.25$, $A = 2$. Insets show the voltage-time dependence at the values of I marked by arrows at which Shapiro steps should appear.

behavior on the Shapiro step in Fig. 4(a), and the nonperiodic one in Fig. 4(b) in its absence.

The situation remains unchanged if more fluxons are introduced. In Fig. 5, the I-V characteristics for two trapped fluxons $M = 2$ at two different values of applied frequencies are presented. As we can see from the I-V characteristic and the corresponding voltage-time dependence in Fig. 5(a), again, Shapiro steps appear in the region, where only two fluxons are present in the system. On the other hand, in Fig. 5(b), where ω is in the region of the $n = 4$ step, i.e., in addition to two trapped fluxons there is also one fluxon-antifluxon pair, there are no Shapiro steps.

When $M = 0$, we could create Shapiro steps anywhere in the I-V characteristic, however, this was not the case for $M \neq 0$. We performed simulations for a wide range of system parameters and obtained that if there were trapped fluxons, regardless of the value of ω or A, Shapiro steps would appear only in the part of the I-V characteristic which corresponds to the step $n = M$ ($n_p = 0$), where only trapped fluxons moved through the AAJJs. If in addition to the trapped fluxons there are also fluxon-antifluxon pairs, i.e., $n = 2n_p + M$ ($n_p \neq 0$), there would be no Shapiro steps. This leads us to the conclusion that the appearance of Shapiro steps is somehow determined by the type of excitations, and raises the question of why for $M \neq 0$ Shapiro steps do not exist if fluxons and fluxon-antifluxon pairs simultaneously circulate in the system.

In order to understand this fact let us consider first the case of one trapped fluxon in the AAJJ. When $M = 1$, in the region of the I-V characteristic, which corresponds to the $n = 1$ step, we have only one circulating fluxon, so it will pass through a junction at the equal time intervals, and consequently, this periodic motion can get locked with some external periodic radiation. In the same way, for any $M \neq 0$ we will have $n = M$ fluxons circulating around the ring equally distributed in space and time. As they move, they are passing through junctions in equal time intervals and this motion can get locked with some external frequency.

However, if in addition to trapped fluxons, we have also fluxon-antifluxon pairs, the situation will be completely different. Let us look at one example: the case of $n = 3$ excitations present in the system. If we have one trapped fluxon and one fluxon-antifluxon pair in which case $n = 2 + 1 = 3$, this will be completely different from the case of 3 trapped fluxons, for which the total number of excitations is also $n = 3$. Three fluxons are always equally distributed in space and time and rotate passing through junctions in the same time intervals. This will change if instead we have two fluxons and one antifluxon. Though they all move periodically, the antifluxon is moving in the opposite direction of the two fluxons, and so they are not any more equally distributed in space and time (the distance between antifluxon and two fluxons is changing as they move). Consequently, they will not pass through a junction at the same time intervals, but the period between two consecutive passages will constantly change, and for that reason, it would be impossible for the system to lock with external radiation.

IV. CONCLUSION

In conclusion, the examination of the fluxon dynamics in an annular array of underdamped Josephson junctions demonstrated that not only the number but also the type of rotating excitations (fluxons or antifluxons) determined the ability of the system to lock with the external radiation. Regardless of the amplitude or frequency of the external radiation, the current-voltage characteristic exhibits Shapiro steps only in the system with trapped fluxons or in the system with fluxon-antifluxon pairs. If the trapped fluxons circulate simultaneously with fluxon-antifluxon pairs, there are *no* Shapiro steps. The obtained results are generic since regardless of system parameters the type of excitations present in the system determines the way the system locks with the external radiation (locking of the external radiation with the Josephson frequency in the case without trapped fluxons or locking with the frequency of circulating fluxons when they are trapped) and most importantly, its ability to exhibit that locking. Though this phenomenon of *missing Shapiro steps* was observed in one particular system, the AAJJ, it could be relevant for any system where dynamics is governed by the moving fluxons and antifluxons since any disbalance between their numbers will change the system behavior. Further investigations certainly require experimental observation of this effect and the settings as in Ref. [14], for instance, could be applied, which would be the subject of our future studies.

Annular Josephson junctions possess an enormous potential for various technological applications. The fluxon dynamics, as well as resonance phenomena, are in the core of some of the most advanced ideas in superconducting digital technologies [1–7]. Another interesting application of annular Josephson junctions is in superconducting metamaterials [29], whose generic element is a superconducting ring split by a Josephson junction. One of the most recent studies has been dedicated to the resonant response of such metamaterials to the external signal in strongly nonlinear regimes [29]. Regardless of the field in which the annular Josephson junctions have the application, a good theoretical guideline and their understanding are crucial. We hope that this work contributes to that understanding and that it will motivate further theoretical and experimental studies.

ACKNOWLEDGMENTS

J.T. wishes to thank the Bogoliubov Laboratory of Theoretical Physics, JINR, Dubna in Russia for their generous hospitality where a part of this work was done. This work was supported by a grant of the fund for developing theoretical physics and mathematics “Bazis.” The reported study was funded by RFBR Research Projects No. 18-02-00318 and No. 18-52-45011-IND, and RSF Project No. 18-71-10095. This work was supported by the Serbian Ministry of Education and Science under Contracts No. OI-171009 and No. III-45010 and by the Provincial Secretariat for High Education and Scientific Research of Vojvodina (Project No. APV 114-451-2201).

[1] J. Clarke, Nature (London) **425**, 133 (2003).
[2] A. Wallraff, A. Lukashenko, J. Lisenfeld, A. Kemp, M. V. Fistul, Y. Koval, and A. V. Ustinov, Nature (London) **425**, 155 (2003).
[3] K. G. Fedorov, A. V. Shcherbakova, M. J. Wolf, D. Beckmann, and A. V. Ustinov, Phys. Rev. Lett. **112**, 160502 (2014).
[4] Q. P. Herr, A. Y. Herr, O. T. Oberg, and A. G. Ioannidis, J. Appl. Phys. **109**, 103903 (2011).
[5] O. A. Mukhanov, IEEE Trans. Appl. Supercond. **21**, 760 (2011).
[6] M. H. Volkmann, A. Sahu, C. J. Fourie, and O. A. Mukhanov, Supercond. Sci. Technol. **26**, 015002 (2013).
[7] N. Takeuchi, Y. Yamanashi, and N. Yoshikawa, Supercond. Sci. Technol. **28**, 015003 (2015).
[8] J. J. Mazo and A. V. Ustinov, *The Sine-Gordon Model and its Applications* (Springer, 2014), pp. 155–175.
[9] O. Braun and Y. S. Kivshar, *The Frenkel-Kontorova Model* (Springer, Berlin, 2003).
[10] J. Tekić and P. Mali, *The ac Driven Frenkel-Kontorova Model* (University of Novi Sad, Novi Sad, 2015).
[11] T. A. Fulton and R. C. Dynes, Solid State Commun. **12**, 57 (1973).
[12] M. Lucci, D. Badoni, V. Merlo, I. Ottaviani, G. Salina, M. Cirillo, A. V. Ustinov, and D. Winkler, Phys. Rev. Lett. **115**, 107002 (2015).
[13] A. Davidson, B. Dueholm, B. Kryger, and N. F. Pedersen, Phys. Rev. Lett. **55**, 2059 (1985).
[14] J. Pfeiffer, A. A. Abdumalikov, Jr., M. Schuster, and A. V. Ustinov, Phys. Rev. B **77**, 024511 (2008).
[15] A. V. Ustinov, M. Cirillo, and B. A. Malomed, Phys. Rev. B **47**, 8357 (1993).
[16] A. V. Ustinov, T. Doderer, R. P. Huebener, N. F. Pedersen, B. Mayer, and V. A. Oboznov, Phys. Rev. Lett. **69**, 1815 (1992).
[17] H. S. J. van der Zant, T. P. Orlando, S. Watanabe, and S. H. Strogatz, Phys. Rev. Lett. **74**, 174 (1995).
[18] A. Wallraff, A. V. Ustinov, V. V. Kurin, I. A. Shereshevsky, and N. K. Vdovicheva, Phys. Rev. Lett. **84**, 151 (2000).
[19] S. Watanabe, S. H. Strogatz, H. S. J. van der Zant, and T. P. Orlando, Phys. Rev. Lett. **74**, 379 (1995).
[20] C. Nappi, M. P. Lisitskiy, G. Rotoli, R. Cristiano, and A. Barone, Phys. Rev. Lett. **93**, 187001 (2004).
[21] R. Monaco, J. Mygind, and V. P. Koshelets, Phys. Rev. B **100**, 064501 (2019).
[22] P. S. Lomdhal, O. H. Soerensen, and P. L. Christiansen, Phys. Scr. **25**, 879 (1982).
[23] H. Kawamoto, Prog. Theor. Phys. **70**, 1171 (1983).
[24] S. Shapiro, Phys. Rev. Lett. **11**, 80 (1963).
[25] A. V. Ustinov, Phys. D (Amsterdam, Neth.) **123**, 315 (1998).
[26] M. V. Fistul, P. Caputo, and A. V. Ustinov, Phys. Rev. B **60**, 13152 (1999).
[27] Y. Shukrinov, I. Rahmonov, and M. Hamdipour, Lect. Notes Comput. Sci. **7125**, 234 (2012).
[28] Y. M. Shukrinov and I. R. Rahmonov, JETP **115**, 289 (2012).
[29] E. I. Kiselev, A. S. Averkin, M. V. Fistul, V. P. Koshelets, and A. V. Ustinov, Phys. Rev. Res. **1**, 033096 (2019).